The stereochemistry of the stable conformational diastereomers in substituted dihydrodibenzo[*ef*,*kl*]heptalenes, the doubly bridged biphenyls. Synthesis, structural elucidation and barrier to conformational diastereomerism †

Parviz Rashidi-Ranjbar,*[a] Ebrahim Kianmehr,[a] Sue-Lein Wang[b] and Fen-Ling Liao[b]

[a] *Department of Chemistry, Faculty of Science, Tehran University, Tehran, Iran*
[b] *Department of Chemistry, The National Tsing-Hua University, Hsinchu, Taiwan, Republic of China*

Received (in Cambridge, UK) 12th October 2001, Accepted 9th January 2002
First published as an Advance Article on the web 8th February 2002

The doubly bridged substituted biphenyls are prepared and separated into the diastereomers by normal chromatography. While in 5,11-dichloro-4,10-dimethoxy-4,10-dihydrodibenzo[*ef*,*kl*]heptalene, **1A**, all the three possible diastereomers, *i.e. endo–endo*; *endo–exo*; and *exo–exo*, are formed; in 5,11-dichloro-4,12-dimethoxy-4,12-dihydrodibenzo[*ef*,*kl*] heptalene, **2A**, only *exo–exo* and *endo–exo* diastereomers could be detected. The diethoxy substituted compounds behave like the methoxy ones, but for the propoxy group, two diastereomers for **1C** and two diastereomers for **2C** are observed. The *endo–endo* diastereomer in **1A** could be converted to the *exo–exo* by a mechanism involving rotation around the pivot bond and a double ring inversion but the reverse process is not observed. The barrier to $\mathbf{1A}_{endo-endo} \longrightarrow \mathbf{1A}_{exo-exo}$ conversion is found to be $\Delta G^{\#}_{403} = 30 \pm 0.3$ kcal mol^{-1} with $\Delta H^{\#}$ of 24.4 ± 0.2 kcal mol^{-1} and $\Delta S^{\#}$ of -14 ± 4 e.u. The structures of the $\mathbf{1A}_{endo-exo}$ and $\mathbf{1A}_{exo-exo}$ isomers and the structure of $\mathbf{2A}_{endo-exo}$ were determined by single crystal X-ray crystallography. Allylic coupling constants are derived for all compounds and compared to the calculated ones. All derivatives having an ethoxy or propoxy group show the CH_2 protons attached to oxygen, diastereotopics.

Introduction

The bridged biphenyls have been studied extensively over a long period of time.[1–11] In many of the investigations, the focus has been on the chiroptical and spectroscopic properties of conformationally restricted biaryls, mostly with a view to the determination of absolute configuration of atropisomeric biaryls.[12–16] We have become interested in this system as a result of the successful separation and determination of conformation and absolute configuration of the conformational diastereomers of *trans*-6,7-disubstituted dibenzo[*a*,*c*]cyclooctene.[17] It was at the same time found that other 6-mono- and *trans*-6,7-disubstituted dibenzo[*a*,*c*]cyclooctenes show a mixture of diastereomeric conformations in solution.[18–20] Recently we have found a new, 2,2′-bridged biphenyl system in which the diastereomeric conformers are observed by ^{1}H-NMR spectroscopy in solution at room temperature.[21] The barrier to conformational conversion should be raised by double bridging of the biphenyl moiety at the 2,2′ and 6,6′ positions such that the conformational diastereomers would be stable enough to be separated and studied. In the present paper we report on the synthesis, separation, structural elucidation and barrier to diastereomeric conversion in substituted dihydrodibenzo-[*ef*,*kl*]heptalenes.

Results and discussion

The di-adduct of the dichlorocarbene-pyrene **3**, Scheme 1, was synthesized as the key compound to prepare the desired compounds. Compound **3** was ring opened in the presence of suitable nucleophilic solvents. It was expected that two structural isomers, **1** and **2** (Scheme 1), each with three possible diastereomers of *exo–exo*, *endo–exo* and *endo–endo*, would be formed. While all possible diastereomers of **1A** and **1B** were formed, only *exo–exo* and *endo–exo* diastereomers of **2A** and

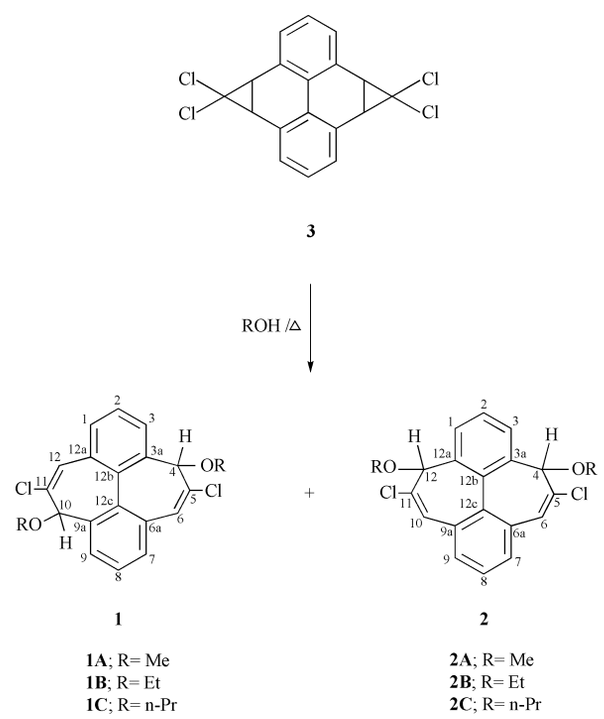

Scheme 1

† Electronic supplementary information (ESI) available: Tables I–III comparing X-ray structural data for $\mathbf{2A}_{endo-exo}$, $\mathbf{1A}_{endo-exo}$ and $\mathbf{1A}_{exo-exo}$ with AM1 calculations. See http://www.rsc.org/suppdata/p2/b1/b109336n/

DOI: 10.1039/b109336n

Table 1 Chemical shifts (in ppm) of the allylic and vinylic protons in substituted **1** and **2** and comparison of the observed and calculated coupling constants (in Hz), according to Sternhell graph[22]

	endo-H			*exo*-H			Vinylic proton
Compound	δ	$^4J_{obs.}$	$^4J_{Cal.}$	δ	$^4J_{obs.}$	$^4J_{Cal.}$	δ
$\mathbf{1A}_{exo-exo}$	4.32	1.5	−1.3	—	—	—	6.64
$\mathbf{1A}_{endo-exo}$	4.30	1.6	−1.3	4.97	2.0	2.3	6.64, 6.84
$\mathbf{1A}_{endo-endo}$	—	—	—	4.88	2.0	2.3	6.67
$\mathbf{2A}_{endo-exo}$	4.12	1.3	−1.3	4.75	2.0	2.3	6.62, 6.83
$\mathbf{2A}_{exo-exo}$	4.15	1.3	−1.3	—	—	—	6.69
$\mathbf{1B}_{exo-exo}$	4.41	1.3	−1.3	—	—	—	6.63
$\mathbf{1B}_{endo-exo}$	4.39	1.5	−1.3	5.05	2.0	2.3	6.61, 6.81
$\mathbf{1B}_{endo-endo}$	—	—	—	5.03	2.0	2.3	6.82
$\mathbf{2B}_{endo-exo}$	4.29	1.5	−1.3	4.91	2.0	2.3	6.67, 6.87
$\mathbf{2B}_{exo-exo}$	4.24	1.2	−1.3	—	—	—	6.67
$\mathbf{1C}_{exo-exo}$	4.39	1.5	−1.3	—	—	—	6.63
$\mathbf{1C}_{endo-exo}$	4.38	1.5	−1.3	5.02	2.0	2.3	6.61, 6.81
$\mathbf{2C}_{endo-exo}$	4.27	1.2	−1.3	4.89	2.0	2.3	6.66, 6.87
$\mathbf{2C}_{exo-exo}$	4.23	1.2	−1.3	—	—	—	6.67

2B were obtained. In the case of propoxy derivatives, the *endo–endo* diastereomers of the **1C** and **2C** structures were not formed, Fig. 1. It was expected that the *endo–endo* diastereomers in each case would form during the ring opening of the starting material, but the barrier of $\mathbf{2}_{endo-endo}$ to $\mathbf{2}_{exo-exo}$ conversion is lower than for the corresponding **1** diastereomers, so that only $\mathbf{2}_{exo-exo}$ will be obtained at the end of the reaction. The same might be true for $\mathbf{1C}_{endo-endo}$. Attempts to convert $\mathbf{2}_{exo-exo}$ to $\mathbf{2}_{endo-endo}$ were not successful, as in **1**, and neither was any $\mathbf{2}_{endo-endo}$ detected from the solvolysis reaction stopped at different intervals.

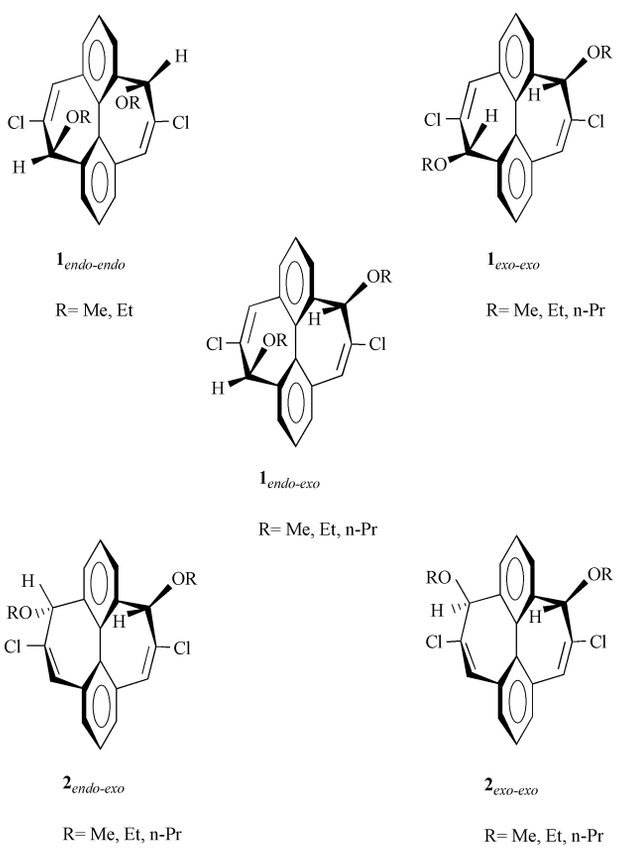

Fig. 1 The diastereomers of **1** and **2** produced by solvolysis.

The fractions obtained by chromatography were recrystallized either in chloroform, chloroform-benzene or ether-ethanol to obtain suitable crystals for X-ray crystallography.

Three samples were considered enough to resolve any ambiguity in the structural elucidation of the geometrical isomers as well as the diastereomers. These will be discussed separately in turn.

$\mathbf{2A}_{endo-exo}$: The crystal of $\mathbf{2A}_{endo-exo}$ belongs to the space group $P2_1/c$; monoclinic. The boat conformation is adopted for seven membered rings with substitutions located at the *endo* and *exo* positions, Fig. 2.

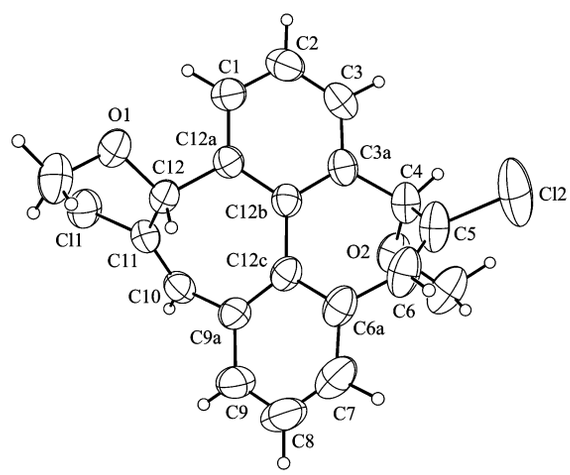

Fig. 2 X-Ray structure of $\mathbf{2A}_{endo-exo}$.

The angle between the planes of the vinylic CH and the allylic C–H bond is found to be −48.9° for the *endo*-H and −175.8° for the *exo*-H. The 500 MHz ^{1}H-NMR spectrum of $\mathbf{2A}_{endo-exo}$ shows two resonances for the allylic (δ = 4.12 and 4.75 ppm) and vinylic protons (δ = 6.62 and 6.83 ppm). The allylic coupling constants (2.0 Hz for *exo*-H and 1.3 Hz for *endo*-H) agree fairly well with the one estimated using the Sternhell[22] graph, Table 1.

Analysis of the structural parameters in $\mathbf{2A}_{endo-exo}$ shows that no local symmetry is retained in the solid state. If we focus on the structural parameters in two seven membered rings; the bond lengths are longer in one and in the other one the bond angles are wider (Table I, supplementary material). The difference in bond lengths of the two double bonds (C10–C11, C5–C6) is 0.01 Å and the difference in bond angles of Csp^2–Csp^3–Csp^2 of the seven membered rings (C10–C11–C12, C6–C5–C4) is 4°, Table 2.

The differences in dihedral angles in the seven membered rings around single bonds (C12c–C9a–C10–C11, C10–C11–C12–C12a, C11–C12–C12a–C12b and C12c–C6a–C6–C5, C6–C5–C4–C3a, C5–C4–C3a–C12b) are about 7°, Table 2. It is interesting to note that dihedral angles in the seven membered ring with longer bond lengths are greater than in the other one.

Table 2 Comparison of selected X-ray structural data with the AM1 calculated values. Bond lengths (Ångstrom), bond angles and dihedral angles (degree)

Compound		X-ray	AM1		X-ray	AM1
2A$_{endo–exo}$						
	Cl1–C11	1.735(2)	1.695	Cl2–C5	1.742(2)	1.704
	C12b–C12c	1.496(3)	1.470	C11–C12	1.524(3)	1.508
	C10–C11	1.323(3)	1.345	C9a–C10	1.478(3)	1.458
	C4–C5	1.519(3)	1.506	C5–C6	1.313(4)	1.342
	O2–C4	1.416(3)	1.430	O1–C12	1.414(2)	1.426
	C10–C11–C12	120.15(19)	118.9	C6–C5–C4	124.2(2)	123.5
	O1–C12–C11–Cl1	17.0	11.8	C12b–C12c–C6a–C6	−6.5	−3.6
	C12b–C12c–C9a–C10	−1.5	−2.2	C12c–C12b–C12a–C12	−1.2	−2.4
	C12c–C12b–C3a–C4	−2.2	−5.6	C12c–C9a–C10–C11	−46.9	−48.2
	C10–C11–C12–C12a	70.4	68	C11–C12–C12a–C12b	−71.8	−71.3
	C12c–C6a–C6–C5	−39.9	−44.3	C6–C5–C4–C3a	63.0	60.3
	C5–C4–C3a–C12b	−64.4	−61.5			
1A$_{endo–exo}$						
	O1–C10	1.413(3)	1.425	C12a–C12b	1.428(3)	1.415
	C12b–C12c	1.497(3)	1.470	C4–C5	1.515(3)	1.505
	Cl2–C5	1.742(2)	1.704	C6–C6a	1.471(3)	1.456
	Cl1–C11	1.739(3)	1.694	C6a–C12c	1.422(3)	1.411
	C12–C12a	1.471(3)	1.458			
	Cl1–C11–C10	117.7(2)	120.2	C4–C3a–C12b	120.4(2)	122.9
	C10–C11–C12	121.1(2)	119.0			
	O1–C10–C11–Cl1	16.6	11.2	C12b–C3a–C4–C5	−71.6	−63.4
	C12–C12a–C12b–C12c	−10.8	4.0	C5–C6–C6a–C12c	−34.4	−42.6
	C11–C12–C12a–C12b	−39.1	−46.1	C6–C6a–C12c–C12b	−13.0	−5.8
	C10–C9a–C12c–C12b	6.1	−1.0	C9a–C10–C11–C12	68.3	68.1
	C12c–C9a–C10–C11	−76.5	−72.2	C3a–C4–C5–C6	63.1	60.1
1A$_{exo–exo}$						
	O1–C10	1.398(5)	1.425	Cl1–C11	1.735(5)	1.694
	O2–C4	1.402(6)	1.425	C10–C9a	1.518(5)	1.506
	C10–C11	1.524(5)	1.508	C4–C5	1.521(4)	1.508
	C11–C12	1.322(5)	1.345	C6–C6a	1.469(6)	1.457
	C5–C6	1.316(6)	1.346	C6a–C12c	1.429(5)	1.412
	C12b–C12c	1.493(4)	1.469	C9a–C12c	1.424(6)	1.413
	Cl2–C5	1.725(5)	1.696			
	O2–C4–C3a	114.7(3)	108.8	C10–C11–C12	121.6(4)	119.2
	O1–C10–C9a	110.6(3)	108.8	O2–C4–C5	110.4(4)	114.2
	Cl1–C11–C10	117.6(3)	120.1	Cl2–C5–C4	117.3(3)	120.1
	O2–C4–C5–Cl2	17.7	12.0	C5–C6–C6a–C12c	−38.9	−45.4
	C12–C12a–C12b–C12c	−10.4	−4.2	C6–C6a–C12c–C12b	−9.0	−3.8
	C11–C12–C12a–C12b	−38.3	−45.2			

While torsions around the three benzene carbon–carbon bonds connected to the bridged carbons (C12b–C12c–C9a–C10, C12c–C12b–C12a–C12, C12c–C12b–C3a–C4) are around −1.5 degree, the fourth one (C12b–C12c–C6a–C6) deviates considerably from planarity by having a torsion of −6.5 degree, Table 2. The structure of **2A**$_{endo–exo}$ calculated by AM1 was compared to the X-ray structure. Bond lengths calculated by AM1, in general, are shorter than the X-ray ones, the most striking one being the C–Cl bond length, Table 2.

1A$_{endo–exo}$: The crystal of **1A**$_{endo–exo}$ belongs to the space group $P2_1/c$; monoclinic. The crystal structure shows that the seven membered rings adopt the boat conformation and the substitutions are located at the *endo* and *exo* positions, Fig. 3.

The angle between the plane of the allylic C–H bond and the plane of the vinylic CH is found to be −47.4 degree for the *endo*-H and −176.3 degree for the *exo*-H. These angles are concerned in establishing the geometry of other diastereomers by analysis of coupling constants.

The 500 MHz ^{1}H-NMR spectrum of **1A**$_{endo–exo}$ shows two resonances for the allylic (δ = 4.30, 4.97 ppm) and vinylic protons (δ = 6.64 and 6.84 ppm). The experimental allylic coupling

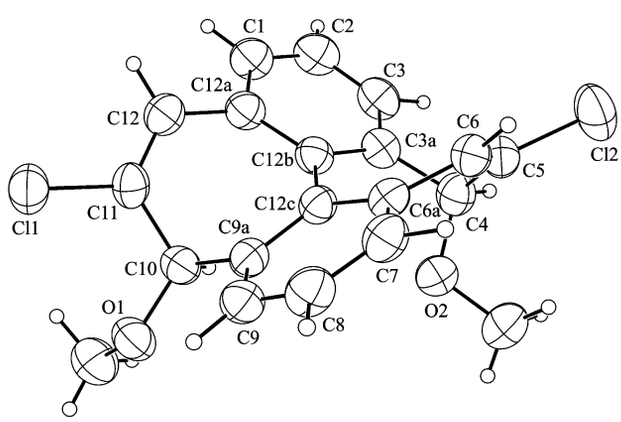

Fig. 3 X-Ray structure of **1A**$_{endo–exo}$.

constants (2.0 Hz for *exo*-H and 1.6 Hz for *endo*-H) are in agreement with the work of Sternhell,[22] Table 1.

The agreement between the calculated coupling constant and the experimental one is fairly good considering the effect of electronegative groups connected to the 4, 5 and 10, 11

positions, the effect of which is not considered in the reported graph.

Analysis of the structural parameters in $\mathbf{1A}_{endo–exo}$ shows that no local symmetry is retained in the solid state. In $\mathbf{1A}_{endo–exo}$, like $\mathbf{2A}_{endo–exo}$, one of the seven membered rings has longer bond lengths but the differences are around 0.005 Å. Also the other seven membered ring shows wider bond angles (Table II, supplementary material). The differences in dihedral angles around the single bonds (C11–C12–C12a–C12b, C9a–C10–C11–C12, C12c–C9a–C10–C11 and C5–C6–C6a–C12c, C3a–C4–C5–C6, C12b–C3a–C4–C5) are about 5 degree, and the ring with longer bond lengths shows greater dihedral angles, Table 2.

$\mathbf{1A}_{exo–exo}$: The crystal of $\mathbf{1A}_{exo–exo}$ belongs to the space group *Cc*; monoclinic. Both the seven membered rings adopt the boat conformation and the substitutions are located at the *exo* positions, Fig. 4.

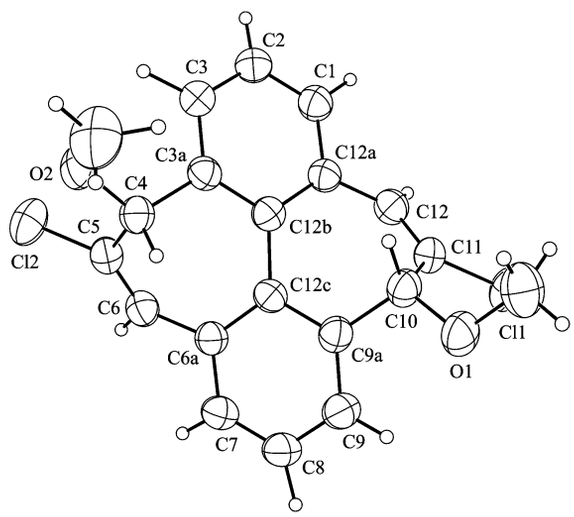

Fig. 4 X-Ray structure of $\mathbf{1A}_{exo–exo}$.

The angle between the allylic C–H bond and the plane of the vinylic CH is found to be −52.5 and −44.7 degree. The 500 MHz ^{1}H-NMR spectrum of $\mathbf{1A}_{exo–exo}$ shows one resonance for the allylic (δ = 4.32 ppm) and vinylic protons (δ = 6.64 ppm). The experimental allylic coupling constant (1.5 Hz) is in agreement with the estimated one, Table 1.

The X-ray structure parameters of $\mathbf{1A}_{exo–exo}$ do not show the same trend compared to $\mathbf{1A}_{endo–exo}$ and $\mathbf{2A}_{endo–exo}$. The differences between the two seven membered rings do not follow a simple trend and the dihedral angles are almost the same (Table III, supplementary material). It seems that the existence of one substituent at the *endo* position in one of the seven membered rings has an effect on the observed differences between the two seven membered rings in $\mathbf{1A}_{endo–exo}$ and $\mathbf{2A}_{endo–exo}$.

Bond lengths of $\mathbf{1A}_{exo–exo}$ calculated by AM1, in general, are shorter than the X-ray ones, Table 2. The bond lengths of both double bonds in the seven membered rings (C5–C6, C11–C12) are calculated to be 0.03 and 0.023 Å longer compared to the X-ray structure ones. The bond connecting the two phenyl rings is calculated to be 0.024 Å shorter than the X-ray structure one. The C–Cl bonds show the most deviations, Table 2.

The structure of $\mathbf{1A}_{endo–endo}$ was unambiguously verified by heating $\mathbf{1A}_{endo–endo}$. ^{1}H-NMR shows that $\mathbf{1A}_{endo–endo}$ is converted to $\mathbf{1A}_{exo–exo}$ under heating in deuterated benzene at 130 °C in a few minutes. Attempts at the conversion of $\mathbf{1A}_{exo–exo}$ to $\mathbf{1A}_{endo–endo}$ starting from a pure sample of $\mathbf{1A}_{exo–exo}$ were not successful; no change in the signals of $\mathbf{1A}_{exo–exo}$ was observed, while heating a pure sample of $\mathbf{1A}_{endo–endo}$ ends up with the $\mathbf{1A}_{exo–exo}$ diastereomer. The ^{1}H-NMR spectrum of $\mathbf{1A}_{endo–endo}$ shows one signal for the allylic (δ = 4.88 ppm) and one for the vinylic proton (δ = 6.67 ppm). The observed coupling constant (J = 2.0 Hz) agrees with the one estimated by the Sternhell method.[22]

The barrier to diastereomeric conversion of $\mathbf{1A}_{endo–endo} \longrightarrow \mathbf{1A}_{exo–exo}$ was studied by heating pure samples of $\mathbf{1A}_{endo–endo}$ at 120, 130 and 140 °C at different intervals in deuterated benzene as solvent. The spectrum of each sample was used to estimate the amount of the other diastereomer. To carry out the kinetic analysis, the reverse reaction was not considered, as heating the pure $\mathbf{1A}_{exo–exo}$ sample did not produce any $\mathbf{1A}_{endo–endo}$ diastereomer. By using the Eyring equation, the activation free energy of $\mathbf{1A}_{endo–endo} \longrightarrow \mathbf{1A}_{exo–exo}$ conversion was found to be $\Delta G^{\#}_{403}$ = 30 ± 0.3 kcal mol^{-1}. Values for $\Delta H^{\#}$ and $\Delta S^{\#}$ are estimated to be 24.4 ± 0.2 kcal mol^{-1} and −14 ± 4 e.u., respectively. The value estimated for $\Delta S^{\#}$ could be explained by adopting simultaneous inversion of both seven membered rings at the T.S. of the ring inversion process, which probably passes *via* a symmetric T.S. compared to the ground state of $\mathbf{1A}_{endo–endo}$. The activation entropy in bridged biphenyl containing one seven membered ring is reported to be $-3 \pm 4 \sim -7 \pm 4$ e.u.[3,23]

Evidence for simultaneous inversion of the rings was obtained from the fact that on heating $\mathbf{1A}_{endo–endo}$, $\mathbf{1A}_{exo–exo}$ was the only product observed and $\mathbf{1A}_{endo–exo}$ was not detected in the high resolution ^{1}H-NMR spectrum with a very high signal to noise ratio.

The ring inversion process in $\mathbf{1A}_{endo–endo}$ was studied by the MMP2 Molecular Mechanics method.[24,25] Different dihedral angles were derived; it was found that inversion of the biphenyl unit could be effected by first driving the C12b–C3a–C4–C5 dihedral angle from −70 to 70 and thereafter the C12c–C9a–C10–C11 dihedral angle from −70 to 70 (for the numbering see Scheme 1). The tentative transition state thus reached was 34 kcal mol^{-1} above the *endo–endo* form.

The structure of $\mathbf{2A}_{exo–exo}$ was established by comparing the chemical shifts of the allylic (δ = 4.15 ppm) and vinylic protons (δ = 6.69 ppm) to the $\mathbf{1A}_{exo–exo}$. The observed coupling constant (J = 1.3 Hz) agrees quite well with the assigned structure.

To judge the observed products ratio for the dimethoxy derivatives, heats of formation were estimated by AM1 for all the diastereomers, Table 3. There is no agreement between the estimated values and the product ratio, if one assumes that the products are formed under the thermodynamic control condition of reaction. The products might be formed under the kinetic control condition, in which the activation energy for the products formation controls the reaction. Efforts to calculate such transition state structures were not successful.

The results of Table 3 reveal that there is correlation between the isomeric ratios and the chain length of the alcohols. The products ratio shows that the diastereoselectivity of the reaction is improved by the use of *n*-propanol which is a better nucleophile.

Experimental

All the materials were received from Merck and used without further purification. ^{1}H- and ^{13}C-NMR spectra were recorded on Varian 500 MHz and Bruker 400 MHz spectrometers. Mass spectra were recorded on VG 7070E or Kratos 2H instruments. Melting points were taken on a Büchi SMP-20 apparatus and are uncorrected.

Crystal structure determination ‡

Crystals of $\mathbf{2A}_{endo–exo}$, $\mathbf{1A}_{endo–exo}$ and $\mathbf{1A}_{exo–exo}$ of dimensions 0.25 × 0.1 × 0.08 mm, 0.42 × 0.41 × 0.3 mm and 0.8 × 0.45 × 0.4 mm, respectively, were selected for indexing and intensity data collection on a Siemens Smart-CCD diffractometer equipped with a normal focus, 3 kW sealed tube X-ray source. Intensity data were collected in 1271 frames with increasing ω (width of

‡ CCDC reference numbers 173087–173089. See http://www.rsc.org/suppdata/p2/b1/b109336n/ for crystallographic files in .cif or other electronic format.

Table 3 The yield of products (%). The number of rotamers and population average of heats of formation (kcal mol^{-1}) for **1A** and **2A** compounds

Compound	Yield	No. of rotamers	H_f	Compound	Yield	Compound	Yield
$\mathbf{2A}_{exo-exo}$	14.3	6	−0.76	$\mathbf{2B}_{exo-exo}$	15.3	$\mathbf{2C}_{exo-exo}$	12.1
$\mathbf{2A}_{endo-exo}$	20.4	9	1.16	$\mathbf{2B}_{endo-exo}$	23.6	$\mathbf{2C}_{endo-exo}$	26.9
$\mathbf{1A}_{exo-exo}$	25.4	6	−1.14	$\mathbf{1B}_{exo-exo}$	22	$\mathbf{1C}_{exo-exo}$	5
$\mathbf{1A}_{endo-exo}$	27.5	9	1.08	$\mathbf{1B}_{endo-exo}$	28.3	$\mathbf{1C}_{endo-exo}$	50.1
$\mathbf{1A}_{endo-endo}$	10.2	6	3.3	$\mathbf{1B}_{endo-endo}$	5.9		

Table 4 Summary of crystal data and intensity collection for $\mathbf{1A}_{endo-exo}$, $\mathbf{1A}_{exo-exo}$ and $\mathbf{2A}_{endo-exo}$

	$\mathbf{1A}_{endo-exo}$	$\mathbf{1A}_{exo-exo}$	$\mathbf{2A}_{endo-exo}$
Empirical formula	$C_{20}H_{16}Cl_2O_2$	$C_{20}H_{16}Cl_2O_2$	$C_{20}H_{16}Cl_2O_2$
Color; shape	Colorless; Equant	Colorless; Columnar	Colorless; Equant
Crystal system	Monoclinic	Monoclinic	Monoclinic
Space group	$P2_1/c$	Cc	$P2_1/c$
Unit cell dimensions	a = 9.5229(2) Å; b = 17.2091(3) Å; β = 95.0960(10)°; c = 10.37020(10) Å	a = 9.8062(7) Å; b = 22.3707(15) Å; β = 115.9140(10)°; c = 8.4900(6) Å	a = 12.3267(3) Å; b = 12.84100(10) Å; β = 111.53°; c = 11.7222(2) Å
Volume/Å^3	1692.76(5)	1675.2(2)	1726.06(5)
Z	4	4	4
Formula weight	359.23	359.2	359.23
Radiation	Mo-Kα (λ = 0.71073 Å)	Mo-Kα (λ = 0.71073 Å)	Mo-Kα (λ = 0.71073 Å)
Temperature/K	293(2)	295	293(2)
Monochromator	Highly oriented graphite crystal	Highly oriented graphite crystal	Highly oriented graphite crystal
Reflections collected	9440 (7445 ≥ 3.0$\sigma(I)$)	9170 (5916 ≥ 3.0$\sigma(I)$)	10033
Independent reflections	3575 (2294 ≥ 3.0$\sigma(I)$) (R(int) = 3.47%)	2330 (2200 ≥ 3.0$\sigma(I)$) (R(int) = 5.27%)	3791 (R(int) = 5.27%)
Final R indices (obs. data)	R = 0.0381, Rw = 0.0420	R = 0.0417, Rw = 0.0507	R = 0.0496, Rw = 0.1188

0.3 deg per frame). Unit cell dimensions were determined by least-squares fits of 2686; 5438 and 4048 reflections, respectively, with $5 < 2\theta < 50$ deg. Absorption correction was based on 3823, 6500, 4176 symmetry-equivalent reflections, respectively, using the SHELXTL-PC program package[26] (Tmin, max = 0.616, 0.920; 0.330, 0.962 and 0.797, 0.930, respectively). On the basis of systematic absences, statistics of intensity distribution, and successful solution and refinement of the structure, the space groups were determined to be $P2_1/c$, $P2_1/c$ and Cc, respectively. Crystal data and information about the intensity collections are given in Table 4.

Computational

Initial estimates of the geometries of structures, for semi-empirical calculations, were obtained by the MMX molecular mechanics method implemented in PCMODEL software.[27] Full minimization was done by using the semiempirical AM1 hamiltonian,[28] implemented in the MOPAC 6.0 program.[29] The MMP2-87 molecular mechanics calculations[24,25] were performed using the interactive computer graphics program MOLBUILD.[30]

General procedure for preparation of 1 and 2 derivatives (Scheme 1)

Dichlorocarbene–pyrene adduct **3** was synthesized according to the published procedure[31] and purified by column chromatography over silica gel using hexane as eluent. **3** was dissolved in suitable alcohol and the solution was heated at 120 °C in a sealed tube for at least two hours. The reaction was followed by TLC. The solvent was evaporated under vacuum. Solvolysis products were separated by alumina PLC using hexane as the mobile phase. Very close bands were separated and subjected to crystallization to obtain the pure fractions.

The barrier for conversion of $\mathbf{1A}_{endo-endo} \longrightarrow \mathbf{1A}_{exo-exo}$ was determined by heating the pure $\mathbf{1A}_{endo-endo}$ isomer. For this purpose samples of $\mathbf{1A}_{endo-endo}$ isomer were dissolved in deuterated benzene and heated in sealed tubes in a thermostatic oil bath. The sealed tubes were taken at different intervals and cooled immediately. Conversion of $\mathbf{1A}_{endo-endo}$ to $\mathbf{1A}_{exo-exo}$ was followed by ^{1}H-NMR by following the changes in signal intensities.

Physical and spectral data

5,11-Dichloro-4,10-dimethoxy-4,10-dihydrodibenzo[*ef*,*kl*]-heptalene ($\mathbf{1A}_{exo-exo}$). Recrystallized from chloroform (colorless crystals, mp 223–224 °C). ^{1}H-NMR ($CDCl_3$, 500 MHz) δ 3.5 (s, 6H), 4.32 (d, J = 1.5 Hz, 2H), 6.64 (d, J = 1.6 Hz, 2H), 7.27 (d, J = 7.7 Hz, 2H), 7.52 (t, J = 7.7 Hz, 2H), 7.61 (d, J = 7.7 Hz, 2H); ^{13}C-NMR ($CDCl_3$, 500 MHz) δ 58.16, 77.14, 119.66, 123.54, 127.31, 127.83, 130.65, 134.53, 135.66, 141.63; MS (EI) m/z 323.0876(M^+ − Cl, 100), 277(19), 273(21), 245(17), 244(95), 236(12), 213(25), 202(18), 201(15), 200(18), 161(9), 149(4), 142(7), 111(3), 100(3), 97(2). Anal. Calcd for $C_{20}H_{16}O_2Cl_2$: C, 67.03; H, 4.50. Found C, 66.91; H, 4.38%.

5,11-Dichloro-4,10-dimethoxy-4,10-dihydrodibenzo[*ef*,*kl*]-heptalene ($\mathbf{1A}_{endo-exo}$). Recrystallized from chloroform-benzene 1 : 1 (colorless crystals, mp 210–211 °C). ^{1}H-NMR ($CDCl_3$, 500 MHz) δ 3.0 (s, 3H), 3.49 (s, 3H), 4.30 (d, J = 1.6 Hz, 1H), 4.97 (d, J = 2 Hz, 1H), 6.64 (d, J = 1.6 Hz, 1H), 6.84 (d, J = 2 Hz, 1H), 7.26 (d, J = 7.3 Hz, 1H), 7.34–7.38 (m, 2H), 7.46–7.51 (m, 2H), 7.59 (d, J = 7.9 Hz, 1H); ^{13}C-NMR ($CDCl_3$, 500 MHz) δ 56.40, 58.49, 77.48, 88.09, 119.84, 123.59, 126.06, 127.28, 127.93, 127.96, 128.00, 129.27, 131.35, 132.29, 133.41, 133.57, 136.28, 136.69, 140.21, 141.38. Anal. Calcd for $C_{20}H_{16}O_2Cl_2$: C, 67.03; H, 4.50. Found C, 66.78; H, 4.42%.

5,11-Dichloro-4,10-dimethoxy-4,10-dihydrodibenzo[*ef*,*kl*]-heptalene ($\mathbf{1A}_{endo-endo}$). Light yellow crystals, mp 119–125 °C (from chloroform). ^{1}H-NMR ($CDCl_3$, 400 MHz) δ 2.82 (s, 6H), 4.88 (d, J = 2 Hz, 2H), 6.67 (d, J = 1.9 Hz, 2H), 6.98 (d, J = 7.6 Hz, 2H), 7.01 (d, J = 7.5 Hz, 2H), 7.09 (t, J = 7.5 Hz, 2H); ^{13}C-NMR ($CDCl_3$, 75 MHz) δ 56.20, 87.88, 125.60, 127.20, 127.36, 128.41, 131.90, 133.94, 134.36, 139.16. Anal. Calcd for $C_{20}H_{16}O_2Cl_2$: C, 67.03; H, 4.50. Found C, 67.11; H, 4.62%.

5,11-Dichloro-4,12-dimethoxy-4,12-dihydrodibenzo[*ef*,*kl*]-heptalene ($\mathbf{2A}_{endo-exo}$). Recrystallized from chloroform-ether 3 : 1 (colorless crystal, mp 175–176 °C).

^{1}H-NMR ($CDCl_3$, 500 MHz) δ 2.83 (s, 3H), 3.38 (s, 3H), 4.12 (d, J = 1.3 Hz, 1H), 4.75 (d, J = 2 Hz, 1H), 6.62 (d, J = 1.6 Hz, 1H), 6.84 (d, J = 2 Hz, 1H), 7.19–7.23 (m, 3H), 7.30 (t, J = 7.6

Hz, 1H), 7.43 (t, J = 7.6 Hz, 1H), 7.62 (d, J = 7.8 Hz, 1H); ^{13}C-NMR ($CDCl_3$, 500 MHz) δ 55.98, 58.21, 76.90, 87.47, 121.44, 123.42, 125.81, 126.39, 126.61, 126.97, 127.07, 127.97, 128.32, 134.21, 134.35, 134.40, 134.76, 135.86, 141.17, 144.44. Anal. Calcd for $C_{20}H_{16}O_2Cl_2$: C, 67.03; H, 4.50. Found C, 67.19; H, 4.44%.

5,11-Dichloro-4,12-dimethoxy-4,12-dihydrodibenzo[*ef*,*kl*]-heptalene (2A$_{exo–exo}$). Light yellow crystals, mp 170–171 °C (from chloroform). ^{1}H-NMR ($CDCl_3$, 500 MHz) δ 3.44 (s, 6H), 4.15 (d, J = 1.3 Hz, 2H), 6.69 (d, J = 1.5 Hz, 2H), 7.31 (d, J = 7.8 Hz, 2H), 7.41 (dd, J = 8.2 and 7 Hz, 1H), 7.51 (t, J = 7.7 Hz, 1H), 7.56 (d, J = 7.3 Hz, 2H); ^{13}C-NMR ($CDCl_3$, 500 MHz) δ 58.25, 77.01, 119.95, 123.06, 126.05, 126.747, 127.223, 128.39, 134.49, 135.29, 136.84, 143.47; MS (EI) m/z 358(M^+, 1.2), 323(M^+ − Cl, 100), 281(10), 277(12), 273(17), 245(16), 244(75), 213(16), 207(11), 200(12), 144(20), 131(10), 106(4), 100(4), 69(28), 40(23). Anal. Calcd for $C_{20}H_{16}O_2Cl_2$: C, 67.03; H, 4.50. Found 66.98; H, 4.59%.

5,11-Dichloro-4,10-diethoxy-4,10-dihydrodibenzo[*ef*,*kl*]-heptalene (1B$_{exo–exo}$). Colorless crystals, mp 234–235 °C (from chloroform). ^{1}H-NMR ($CDCl_3$, 500 MHz) δ 1.31 (t, J = 7 Hz, 6H), 3.49 (qd, J = 9 and 7 Hz, 1H), 3.74 (qd, J = 9 and 7 Hz, 1H), 4.41 (d, J = 1.3 Hz, 2H), 6.63 (d, J = 1.5 Hz, 2H), 7.25 (d, J = 6.6 Hz, 2H), 7.51 (t, J = 7.7 Hz, 2H), 7.66 (d, J = 6.6 Hz, 2H); ^{13}C-NMR ($CDCl_3$, 125 MHz) δ 15.14, 66.072, 75.44, 119.92, 123.45, 127.26, 127.80, 130.66, 134.54, 136.37, 142.12; MS (EI) m/z 386.0897(M^+, 0.8), 351.11421(M^+ − Cl, 100), 323(7.2), 287(24), 277(22), 259(16), 258(13), 249(10), 236(20), 230(17), 213(20), 203(28), 202(60) 200(22), 161(14), 142(12), 111(4), 82(4). Anal. Calcd for $C_{22}H_{20}O_2Cl_2$: C, 68.38; H, 5.22. Found C, 68.21; H, 5.15%.

5,11-Dichloro-4,10-diethoxy-4,10-dihydrodibenzo[*ef*,*kl*]-heptalene (1B$_{endo–exo}$). Colorless crystals, mp 169–170 °C (from chloroform). ^{1}H-NMR ($CDCl_3$, 500 MHz) δ 0.71 (t, J = 7 Hz, 3H), 1.28 (t, J = 7 Hz, 3H), 3.14 (qd, J = 9.1 and 7 Hz, 1H), 3.22 (qd, J = 9.1 and 7 Hz, 1H), 3.50 (qd, J = 9.1 and 7 Hz, 1H), 3.65 (qd, J = 9.1 and 7 Hz, 1H), 4.3 (d, J = 1.5 Hz, 1H), 5.05 (d, J = 2 Hz, 1H), 6.61 (d, J = 1.5 Hz, 1H), 6.81 (d, J = 2 Hz, 1H), 7.20–7.24 (dd, J = 7.7 and 1.2 Hz, 1H), 7.31 (m, 2H), 7.44 (m, 2H), 7.59 (dd, J = 7.7 and 1.1 Hz, 1H); ^{13}C-NMR ($CDCl_3$, 125 MHz) δ 14.58, 15.04, 63.38, 65.73, 75.23, 85.69, 119.56, 122.82, 125.23, 126.56, 127.23, 127.37, 127.41, 128.63, 131.07, 131.94, 133.05, 133.41, 135.92, 136.90, 140.19, 141.38; MS (EI) m/z 351.1193(M^+ − Cl, 100), 302(13), 287(41), 277(26), 259(19), 258(15), 249(12), 236(22), 230(21), 213(35), 211(13), 203(37), 202(72), 201(20), 200(22), 161(27), 149(10), 142(21), 111(6), 97(6), 57(11). Anal. Calcd for $C_{22}H_{20}O_2Cl_2$: C, 68.38; H, 5.22. Found C, 68.52; H, 5.12%.

5,11-Dichloro-4,10-diethoxy-4,10-dihydrodibenzo[*ef*,*kl*]-heptalene (1B$_{endo–endo}$). Light yellow crystals, mp 117–122 °C (from chloroform). ^{1}H-NMR ($CDCl_3$, 200 MHz) δ 0.7 (t, J = 7 Hz, 6H), 3.05–3.2 (m, 4H), 5.03 (d, J = 2 Hz, 2H), 6.82 (d, J = 2 Hz, 2H), 7.25–7.5 (m, 6H); ^{13}C-NMR ($CDCl_3$, 50 MHz) δ 14.50, 63.31, 85.52, 123.05, 125.46, 127.24, 127.86, 131.10, 133.25, 135.55, 140.46. Anal. Calcd for $C_{22}H_{20}O_2Cl_2$: C, 68.38; H, 5.22. Found C, 68.18; H, 5.33%.

5,11-Dichloro-4,12-diethoxy-4,12-dihydrodibenzo[*ef*,*kl*]-heptalene (2B$_{exo–exo}$). Light yellow crystals, mp 165–166 °C (from chloroform). ^{1}H-NMR ($CDCl_3$, 500 MHz) δ 1.27 (t, J = 7 Hz, 6H), 3.43 (qd, J = 9 and 7 Hz, 2H), 3.66 (qd, J = 9 and 7 Hz, 2H), 4.24 (d, J = 1.2 Hz, 2H), 6.67 (d, J = 1.5 Hz, 2H), 7.29 (d, J = 7.6 Hz, 2H), 7.39 (dd, J = 8.2 and 7 Hz, 1H), 7.54 (dd, J = 8.2 and 7.2 Hz, 1H), 7.63 (d, J = 7.7 Hz, 2H); ^{13}C-NMR ($CDCl_3$, 125 MHz) δ 15.031, 66.01, 75.21, 120.11, 122.81, 125.89, 127.08, 128.21, 135.27, 137.53, 143.81; MS (EI) m/z 351(M^+ − Cl, 100), 287(21), 277(18), 259(16), 258(13), 236(13), 230(14), 213(14), 203(17), 202(38), 201(12), 200(10), 119(4), 69(10). Anal. Calcd for $C_{22}H_{20}O_2Cl_2$: C, 68.38; H, 5.22. Found C, 68.12; H, 5.28%.

5,11-Dichloro-4,12-diethoxy-4,12-dihydrodibenzo[*ef*,*kl*]-heptalene (2B$_{endo–exo}$). Colorless crystals, mp 153–154 °C (from chloroform). ^{1}H-NMR ($CDCl_3$, 500 MHz) δ 0.63 (t, J = 7 Hz, 3H), 1.27 (t, J = 7 Hz, 3H), 3.00 (qd, J = 9 and 7 Hz, 1H), 3.14 (qd, J = 9 and 7 Hz, 1H), 3.43 (qd, J = 9 and 7 Hz, 1H), 3.67 (qd, J = 9 and 7 Hz, 1H), 4.29 (d, J = 1.5 Hz, 1H), 4.91 (d, J = 2 Hz, 1H), 6.67 (d, J = 1.5 Hz, 1H), 6.87 (d, J = 2 Hz, 1H), 7.23–7.27 (m, 3H), 7.34 (t, J = 7.6 Hz, 1H), 7.47 (t, J = 7.5 Hz, 1H), 7.71–7.73 (m, 1H); ^{13}C-NMR ($CDCl_3$, 125 MHz) δ 14.53, 15.06, 63.24, 65.98, 75.142, 85.46, 121.60, 123.25, 125.57, 125.92, 126.26, 126.62, 126.80, 127.84, 128.18, 134.40, 134.58, 134.65, 134.80, 136.52, 141.48, 144.88; MS (EI) m/z 351.11722 (M^+ − Cl, 100), 287(40), 279(23), 278(14), 277(68), 259(24), 249(19), 248(11), 236(20), 214(12), 213(36), 203(31), 202(67), 201(20), 200(16), 161(12), 142(9), 111(2), 85(3). Anal. Calcd for $C_{22}H_{20}O_2Cl_2$: C, 68.38; H, 5.22. Found C, 68.22; H, 5.16%.

5,11-Dichloro-4,10-dipropoxy-4,10-dihydrodibenzo[*ef*,*kl*]-heptalene (1C$_{exo–exo}$). Light yellow crystals, mp 172–173 °C (from chloroform). ^{1}H-NMR ($CDCl_3$, 500 MHz) δ 1.00 (t, J = 7.4 Hz, 6H), 1.69–1.74 (m, 4H), 3.40 (td, J = 8.8 and 6.6 Hz, 2H), 3.65 (td, J = 8.8 and 6.6 Hz, 2H), 4.39 (d, J = 1.5 Hz, 2H), 6.63 (d, J = 1.6 Hz, 2H), 7.25 (d, J = 7.7 Hz, 2H), 7.51 (t, J = 7.7 Hz, 2H), 7.66 (d, J = 7.7 Hz, 2H); ^{13}C-NMR ($CDCl_3$, 125 MHz) δ 10.63, 22.99, 72.18, 75.46, 119.89, 123.38, 127.18, 127.73, 130.63, 134.52, 136.45, 142.19; MS (EI) m/z 379.14626 (M^+ − Cl, 77), 339(22), 338(14), 337(65), 301(19), 279(23), 278(12), 277(49), 260(13), 259(65), 258(14), 251(13), 249(37), 236(19), 231(36), 230(28), 215(17), 214(14), 213(33), 204(12), 203(76), 202(100), 200(19), 91(12). Anal. Calcd for $C_{24}H_{24}O_2Cl_2$: C, 69.54; H, 5.84. Found C, 69.67; H, 5.90%.

5,11-Dichloro-4,10-dipropoxy-4,10-dihydrodibenzo[*ef*,*kl*]-heptalene (1C$_{endo–exo}$). Light yellow crystals, mp 111–112 °C (from chloroform). ^{1}H-NMR ($CDCl_3$, 500 MHz) δ 0.31 (t, J = 7.4 Hz, 3H), 0.96 (t, J = 7.4 Hz, 3H), 1.10–1.17 (m, 2H), 1.64–1.71 (m, 2H), 3.08 (td, J = 8.7 and 6 Hz, 1H), 3.14 (td, J = 8.7 and 6.5 Hz, 1H), 3.38 (td, J = 9 and 6.6 Hz, 1H), 3.56 (td, J = 9 and 6.6 Hz, 1H), 4.38 (d, J = 1.5 Hz, 1H), 5.02 (d, J = 2 Hz, 1H), 6.61 (d, J = 1.5 Hz, 1H), 6.81 (d, J = 2 Hz, 1H), 7.21 (dd, J = 7.7 and 1.1 Hz, 1H), 7.30–7.33 (m, 2H), 7.43 (t, J = 7.5 Hz, 1H), 7.44 (t, J = 7.7 Hz, 1H), 7.59 (dd, J = 7.7 and 1.1 Hz, 1H); ^{13}C-NMR ($CDCl_3$, 125 MHz) δ 9.93, 10.51, 22.50, 22.89, 69.72, 71.99, 75.38, 86.02, 119.67, 122.80, 125.20, 126.65, 127.21, 127.38, 128.62, 131.13, 131.98, 133.03, 133.43, 135.95, 137.07, 140.28, 141.57. HRMS calcd for $C_{24}H_{24}O_2Cl_2$ 414.11544, found 414.11519.

5,11-Dichloro-4,12-dipropoxy-4,12-dihydrodibenzo[*ef*,*kl*]-heptalene (2C$_{exo–exo}$). Light yellow crystals, mp 114–115 °C (from chloroform). ^{1}H-NMR ($CDCl_3$, 500 MHz) δ 0.96 (t, J = 7.5 Hz, 6H), 1.64–1.70 (m, 4H), 3.32 (td, J = 8.8 and 6.5 Hz, 2H), 3.58 (td, J = 8.8 and 6.5 Hz, 2H), 4.23 (d, J = 1.2 Hz, 2H), 6.67 (d, J = 1.6 Hz, 2H), 7.29 (dd, J = 7.7 and 0.5 Hz, 2H), 7.40 (dd, J = 8.2 and 7.0 Hz, 1H), 7.54 (dd, J = 8.2 and 7.2 Hz, 1H), 7.64 (dd, J = 5.7 and 0.32 Hz, 2H); ^{13}C-NMR ($CDCl_3$, 125 MHz) δ 10.60, 22.92, 72.21, 75.30, 120.12, 122.82, 125.88, 126.52, 127.08, 128.21, 134.56, 135.29, 137.65, 143.88; MS (EI) m/z 379.14824 (M^+ − Cl, 100), 337(14), 301(24), 277(45), 259(38), 251(25), 250(19), 249(70), 215(17), 214(11), 213(28), 203(21), 202(39), 201(11), 200(11), 189(7), 106(7), 43(13). Anal. Calcd for $C_{24}H_{24}O_2Cl_2$: C, 69.54; H, 5.84. Found C, 69.43; H, 5.97%.

5,11-Dichloro-4,12-dipropoxy-4,12-dihydrodibenzo[*ef*,*kl*]-heptalene (2C$_{endo–exo}$). Light yellow crystals, mp 107–108 °C

(from chloroform). ^{1}H-NMR ($CDCl_3$, 500 MHz) δ 0.28 (t, J = 7.4 Hz, 3H), 0.97 (t, J = 7.4 Hz, 3H), 1.00–1.14 (m, 2H), 1.64–1.71 (m, 2H), 2.94 (td, J = 8.7 and 6.1 Hz, 1H), 3.07 (ddd, J = 8.7, 6.9 and 5.9 Hz, 1H), 3.32 (td, J = 8.8 and 6.6 Hz, 1H), 3.60 (td, J = 8.6 and 6.5 Hz, 1H), 4.27 (d, J = 1.2 Hz, 1H), 4.89 (d, J = 2 Hz, 1H), 6.66 (d, J = 1.6 Hz, 1H), 6.87 (d, J = 2 Hz, 1H), 7.22–7.30 (m, 3H), 7.32 (t, J = 7.6 Hz, 1H), 7.47 (t, J = 7.6 Hz, 1H), 7.73 (d, J = 7.8 Hz, 1H); ^{13}C-NMR ($CDCl_3$, 125 MHz) δ 10.03, 10.61, 22.39, 22.93, 69.68, 72.17, 75.22, 85.87, 121.63, 123.19, 125.57, 125.97, 126.48, 126.70, 126.81, 127.88, 128.16, 134.36, 134.62, 134.81, 134.86, 136.70, 141.48, 145.03; MS (EI) *m/z* 379.14818 (M^+ − Cl, 80), 302(10), 301(47), 278(25), 277(100), 260(21), 259(88), 249(23), 248(10), 236(14), 214(13), 213(30), 203(41), 202(59), 201(14), 200(11), 189(5), 84(20). Anal. Calcd for $C_{24}H_{24}O_2Cl_2$: C, 69.54; H, 5.84. Found C, 69.36; 5.72%.

Acknowledgements

Parviz Rashidi Ranjbar is grateful to the Research Council of Tehran University for financial support. We thank Professor Tony Durst (University of Ottawa) for providing us access to NMR and HRMS facilities.

References

1 K. Mislow, M. A. W. Glass, H. B. Hopps, E. Simon and G. H. Wahl, *J. Am. Chem. Soc.*, 1964, **86**, 1710.
2 C. Jaime and J. Font, *J. Org. Chem.*, 1990, **55**, 2637–2644.
3 K. Mullen, W. Heinz, F.-G. Klarner, W. R. Roth, I. Kindermann, O. Adamczak, M. Wette and J. Lex, *Chem. Ber.*, 1990, **123**, 2349–2371.
4 J. E. Schulz, K. Rissanen and F. Voegtle, *Chem. Ber.*, 1992, **125**, 2239.
5 I. O. Sutherland and M. V. J. Ramsay, *Tetrahedron*, 1965, **21**, 3401–3408.
6 K. Mislow, M. A. W. Glass, R. E. Brien, P. Rutkin, D. H. Steinberg, J. Weiss and C. Djerassi, *J. Am. Chem. Soc.*, 1962, **84**, 1455–1478.
7 E. Bunnenberg, C. Djerassi, K. Mislow and A. Moscowitz, *J. Am. Chem. Soc.*, 1962, **84**, 2823–2826.
8 K. Mislow, E. Bunnenberg, R. Records, K. Wellman and C. Djerassi, *J. Am. Chem. Soc.*, 1963, **85**, 1342–1349.
9 H. Joshua, R. Gans and K. Mislow, *J. Am. Chem. Soc.*, 1968, **90**, 4884–4892.
10 C. P. Brock and R. P. Minton, *J. Am. Chem. Soc.*, 1989, **111**, 4586–4593.
11 Y. Takei, T. Yamaguchi, Y. Osamura, K. Fuke and K. Kaya, *J. Phys. Chem.*, 1988, **92**, 577–581.
12 K. Mislow, M. A. W. Glass, R. E. O. Brien, P. Rutkin, D. H. Steinberg, J. Weiss and C. Djerassi, *J. Am. Chem. Soc.*, 1962, **84**, 1455.
13 E. Bunnenberg, C. Djerassi, K. Mislow and A. Moscowitz, *J. Am. Chem. Soc.*, 1962, **84**, 2823.
14 K. Mislow, E. Bunnenberg, R. Records, K. Wellman and C. Djerassi, *J. Am. Chem. Soc.*, 1963, **85**, 1342.
15 K. Mislow and J. G. Berger, *J. Am. Chem. Soc.*, 1962, **84**, 1965.
16 A. Moscowitz, K. Mislow, M. A. W. Glass and C. Djerassi, *J. Am. Chem. Soc.*, 1962, **84**, 1945.
17 B. Borecka, S. Cameron, P. Rashidi-Ranjbar and J. Sandstrom, *J. Am. Chem. Soc.*, 1990, **112**, 1185.
18 P. Rashidi-Ranjbar and J. Sandstrom, *J. Chem. Soc., Perkin Trans. 2*, 1990, 901.
19 R. Isaksson, P. Rashidi-Ranjbar and J. Sandstrom, *J. Chem. Soc., Perkin Trans. 1*, 1991, 1147.
20 P. Rashidi-Ranjbar, J. Najafpour and F. Piri, *J. Phys. Org. Chem.*, 1998, **11**, 781–786.
21 P. Rashidi-Ranjbar, S. Taghvaei-Ganjali, S.-L. Wang, F.-L. Liao and A. Heydari, *J. Chem. Soc., Perkin Trans. 2*, 2001, 1255–1260.
22 S. Sternhell, *Quart. Rev.*, 1969, **23**, 236.
23 M. Oki, H. Iwamura and G. Yamamoto, *Bull. Chem. Soc. Jpn.*, 1971, **44**, 262.
24 U. Burkert and N. L. Allinger, *Molecular Mechanics*, American Chemical Society, Washington, DC, 1982.
25 T. Liljeforts, J. Tai, S. Li and L. Allinger, *J. Comput. Chem.*, 1987, **8**, 1051; *Program available from Quantum Chemistry Program Exchange*, Indiana University, Bloomington, IN.
26 G. M. Sheldrick, SHELXTL-plus Crystallographic System, version 4, Analytical International Inc., Madison, WI, USA, 1990.
27 Serena Software, PO Box 3076, Bloomington, IN.
28 M. J. S. Dewar, E. G. Zeobish, E. F. Healy and J. J. P. Stewart, *J. Am. Chem. Soc.*, 1985, **107**, 3902.
29 J. J. P. Stewart, *QCPE 581*, Department of Chemistry, Indiana University, Bloomington, IN.
30 T. Liljefors, *J. Mol. Graphics*, 1983, **1**, 111.
31 J. Hohn, J. Pickardt and P. Weyerstahl, *Chem. Ber.*, 1983, **116**, 798–807.